

On the Longitudinal Striations of Stony Meteorites

Robert F. Weiss, ScD¹

Technology Transitions, Boston, MA 02115, USA

Many recovered stony (glassy) meteorites exhibit longitudinal (streamwise) striations originating at the stagnation point and extending over the entire object. It has been conjectured that such striations are the result of a Lamb-Taylor instability of the molten layer that forms during atmospheric re-entry and experiences thousands of g's of deceleration. This paper suggests that the striations are instead a manifestation of a Görtler-Taylor aerodynamic instability originating in the stagnation region boundary layer and the associated azimuthally periodic shear stress and heat transfer. In the present study, axially symmetric frozen oil models designed to simulate the viscosity- temperature behavior of silicates, are exposed to a free jet at transonic speeds. Extremely steady striations are generated for free-stream Reynolds numbers, and related Görtler numbers, beyond a critical value. The azimuthal wavelengths of the striations, and their dependence on Reynolds number, are in approximate agreement with the wave number of the most amplified disturbance predicted by boundary layer stability analysis. Moreover, the striation wave number on a hemisphere cylinder oil model is in substantial agreement with both the theory and the pattern observed on the Lafayette (Purdue) meteorite.

¹ President; AIAA Associate Fellow.

I.Introduction

P

REVIOUS studies by Feldman [1, 2] have considered the Lamb-Taylor (L-T) inertial instability of a molten glass surface layer, modelled by Bethe and Adams [3], induced by deceleration during re-entry into the atmosphere as the origin of longitudinal striations seen on recovered stony (glassy) meteorites. One example of this class is pictured in Fig. 1.

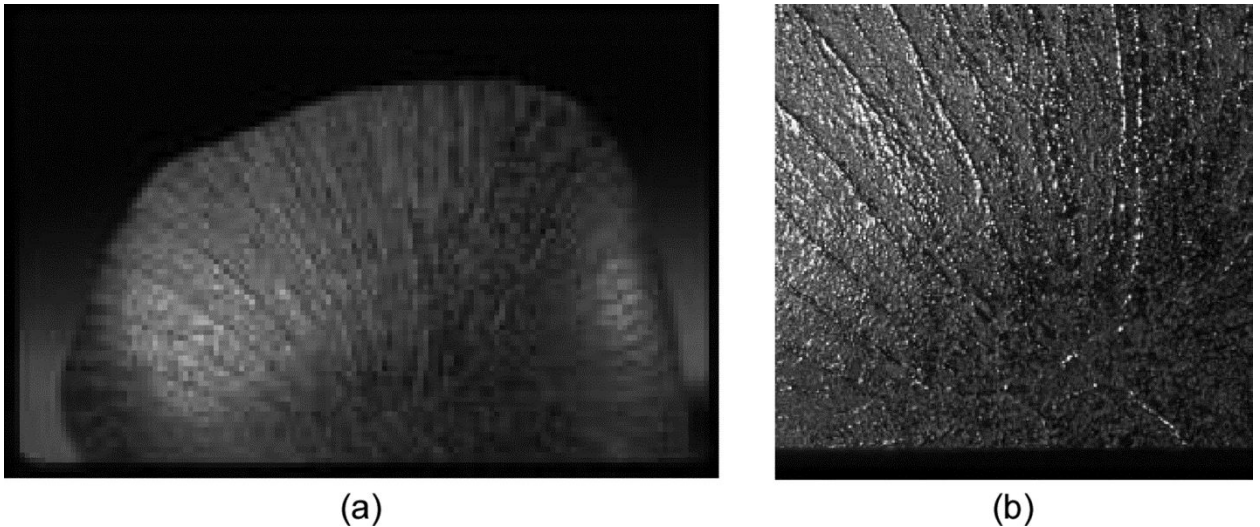


Fig. 1- (a) Lafayette Purdue Nakhite meteorite with longitudinal striations, (b) close-up of the stagnation region (courtesy, The Smithsonian Institute; Chip Clark photo).

While such instabilities are a potential explanation for the striations, Feldman [2] determined that for glassy heat-shields with the properties of Pyrex in a typical re-entry “amplification is negligible during most of the trajectory, and that no liquid will be lost due to L-T instability”. We will demonstrate an alternative Görtler-Taylor (G-T) aerodynamic instability that has created similar striations in transonic flow experiments. These previously unpublished experiments are the subject of this note.

Recovered iron meteorites do not exhibit longitudinal striations, but Williams [5] speculated that a “bound vortex” in the flow is the cause of horseshoe-shaped pits in the ablating surface. Tobak [6] suggested that “cross-hatching” of ablated surfaces on recovered slender re-entry vehicles may have been triggered by the presence of longitudinal vortices, although the resulting patterns are aligned with oblique shock waves. A critical review of the “cross-hatching” phenomenon, and its important effect on vehicle roll dynamics, has been provided by Swigart [7]. Stock [8] then differentiated “streamwise grooves, believed to be created by streamwise vortices situated in the boundary layer and which locally increase heat and mass transfer rates”, from cross-hatching patterns, although both “have been shown to exist in supersonic, laminar, transitional and turbulent boundary layers”.

Many hundreds of studies have examined G-T instabilities, in both attached and separated flows with streamline curvature, under all flight regimes. Petitjean and Westfried [9] analysed the instability in a duct with high curvature, the stagnation points examined in the present study being the singular limit. A recent analysis by Sescu [10] of active flight control algorithms to control G-T vortices is indicative of continuing research in this important area, and broad reviews of G-T phenomena by Floryan [11] and Saris [12] are available. An important application is the prediction of boundary layer reattachment on swept wings using advanced numerical methods employed by Hall et al. [13] and LeDuc et al. [14].

Smith and Kuethe [15], Kestin and Wood [16, 17], and Wilson [18] have identified G-T instabilities as a possible source of turbulence detected in the stagnation region of blunt objects. The G-T instability occurs independently of inertial forces on molten layers, or even the existence of molten layers. However, when such layers exist, they would be expected to respond to this instability and its associated span-wise or azimuthally periodic shear stresses and heat transfer rates. A schematic cross-section of such longitudinal vortex streamlines, reproduced from Kestin and Wood [17], is illustrated in Fig. 2.

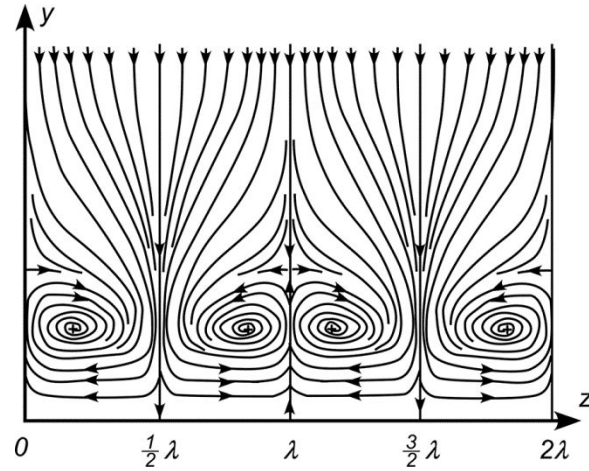


Fig. 2 - Cross-section of streamlines in counter-rotating vortices due to a Görtler-Taylor stagnation region instability; reproduced from Ref. [17]. The upward pointing streamlines are in locations where molten layer striations would be expected to form. Their spacing (wavelength) equals twice the vortex diameter.

The characteristic length scale for a vortex array embedded in a stagnation region boundary layer is obviously the local boundary layer thickness. Assuming to first order that the vortex array wavelength is twice the axisymmetric stagnation point boundary layer thickness δ [19], as suggested by Fig. 2, the ratio of wavelength to body radius is then:

$$\lambda/R \sim 2 (\delta / R) = 2(2.4 \text{ Re}^{-1/2}) = 4.8 \text{ Re}^{-1/2} \quad (1)$$

Where Re is the Reynolds number based on body radius. As experimentally observed and described in the following sections, the initial stagnation region striations spread azimuthally as they flow downstream, leaving space for new vortex pairs at the transition from hemisphere to cylinder, with the result that the number of striations scales with the local cross-sectional radius.

The small disturbance stability analysis of Kestin and Wood [17] for a stagnation line boundary layer yielded the following relationship (Eq. 14 C) between a “unique disturbance wavelength”, body radius R and Reynolds Number:

$$\lambda/R = 2(1.79 \pi \text{ Re}^{-1/2}) = 11.2 \text{ Re}^{-1/2} \quad (2)$$

II. Experimental Methods

Initially frozen SAE # 10 oil hemisphere-cylinder models were tested in a circular free jet. These were molded by a cavity in a block of dry ice formed with a hot steel mandrel, and a central support rod was frozen within it. In a few test runs, a single thermocouple was inserted to record its exposure to the free stream and provide a rough estimate of melt removal rate.

The models were rapidly positioned before a run began and before any surface melting commenced. Instrumentation consisted of pitot-static tubes to check stagnation pressure and Mach number, and photographic equipment to record the appearance of any flowing oil during a test. The test gas was dry nitrogen supplied by a tank farm that provided up to two minutes of test time. Tank gas was at room temperature (20 deg. C), and dropped to an ambient temperature of approximately 16 deg. C at transonic speeds. Heat transfer to the model was driven by the difference between the stagnation temperature of 20 deg. C and an initial temperature of -78 deg. C of oil that had been frozen for 24 hours in dry ice.

III. Axi-Symmetric Stagnation Flow Experiments

At the maximum ($M = 0.8$) velocities of these tests, $Re \sim 140,000$, where it is generally assumed that stagnation region flows are turbulent. However, vortex formation and stretching can occur before transition to a fully turbulent flow significantly downstream. This is the behavior seen in the flow between concentric rotating cylinder experiments of Taylor, as described by Schlichting [19]. Vortices were first seen at $Re = 94.5$ (based on the velocity of the inner cylinder and gap dimension) and a Taylor number $T = Re (d/R)^{1/2} > 41.3$, with fully turbulent vortices not appearing until $Re = 3960$ and $T = 1715$.

Vortex formation and breakdown will ultimately lead to turbulence. It is important to recognize, however, that stagnation region G-T vortices are macroscopic structures totally different than the random fluctuations in fully turbulent flow. In free shear flows such as hypersonic wakes, it has been shown by Legner and Finson [20] that small scale turbulence actually stabilizes wake growth, acting as an enhanced viscosity. The same effect may be present in G-T vortices at higher Reynolds number.

As the temperature at the jet flow-model interface increased due to the difference between the stagnation temperature (room temperature in these experiments) and that of the initially frozen oil, a stable molten layer formed, its thickness dependent on the inverse viscosity-temperature relationship. Under transonic flow conditions, remarkably stable longitudinal striation patterns were generated in the ensuing molten layer. Photos taken during these experiments, presented in Figures 3 and 4, were conducted at increasing stagnation pressure and Reynolds number, resulting in increased model ablation and molten layer interface velocities, as summarized in Table I and compared to a calculation of a typical blunt re-entry body trajectory [2].

Table 1 – Comparison of test conditions with typical re-entry conditions

Conditions for a typical re-entry body [2]		Test conditions for a 5 cm frozen oil hemisphere-cylinder	SAE # 10
Re-entry Mach number & Post-shock velocity	M = 22 V = 450 m/sec	Maximum jet flow Mach number and velocity	M = 0.8 V = 300 m/sec
Stagnation pressure; Reynolds number	1.2 atm 196,000	Stagnation pressure range; Reynolds number range	2 – 4 atm; 100 – 200,000
Stagnation temperature; Initial surface temperature at peak heating	3500 deg K 2500 deg K	Stagnation temperature; Initial surface temperature	20 deg C; -78 deg C
Kinematic viscosity - temperature exponent; Calculated liquid layer thickness; & Layer velocity at peak heating	0.04 (cgs); n = 11; 0.002 cm 100 cm/sec	Kinematic viscosity - temperature exponent; Calculated liquid layer thickness; Layer velocity	0.02 (cgs); n = 5.5; 0.006 cm; 25 cm/sec
Time to peak heating & Maximum deceleration from 100 Km	24 sec; 27 sec.	Test time available	2 minutes

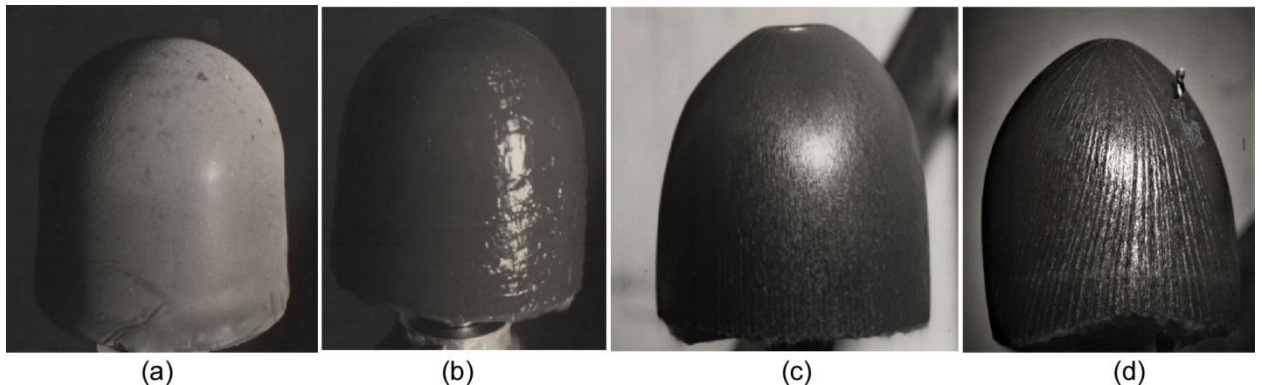


Fig. 3-Transonic flow tests.

(a) frozen oil model; (b) axially propagating waves at lowest stagnation pressure and Reynolds number; (c) onset of longitudinal striations at “critical” Reynolds number; (d) highest Reynolds number test (140,000, based on model radius) with model at a slight angle-of-attack; note that longitudinal striations follow the streamlines and surface shear stresses produced by boundary layer vortices.

In panel (b), typical Rayleigh surface waves were seen. As the stagnation pressure of the free jet was increased, stationary azimuthally periodic grooves and striations are visible in panel (c), but were not prominent until the critical Reynolds Number of 140,000 was reached and exceeded. Note in panel (d) how the striations follow the

external flow streamlines at the small angle-of-attack experienced late in a test. Stable structures that form at even higher Reynolds numbers are consistent with counter-rotating G T vortices and the associated increased heat transfer/shear stress within them. The “valleys” of these structures appear to become deeper and their accompanying ridges higher as the molten layer thickens downstream with the transport of material from valleys to ridges. The observed striations are azimuthally periodic, with their relatively sharp peaks and flat valleys similar to the striations seen on stony meteorites. They clearly follow the ambient flow streamlines, indicating that they are driven by local shear stresses at the flow-oil interface. Photos of the model taken during a test were used to estimate the number visible close to the stagnation point, at the hemisphere- cylinder transition, and at the trailing edge of the cylinder.

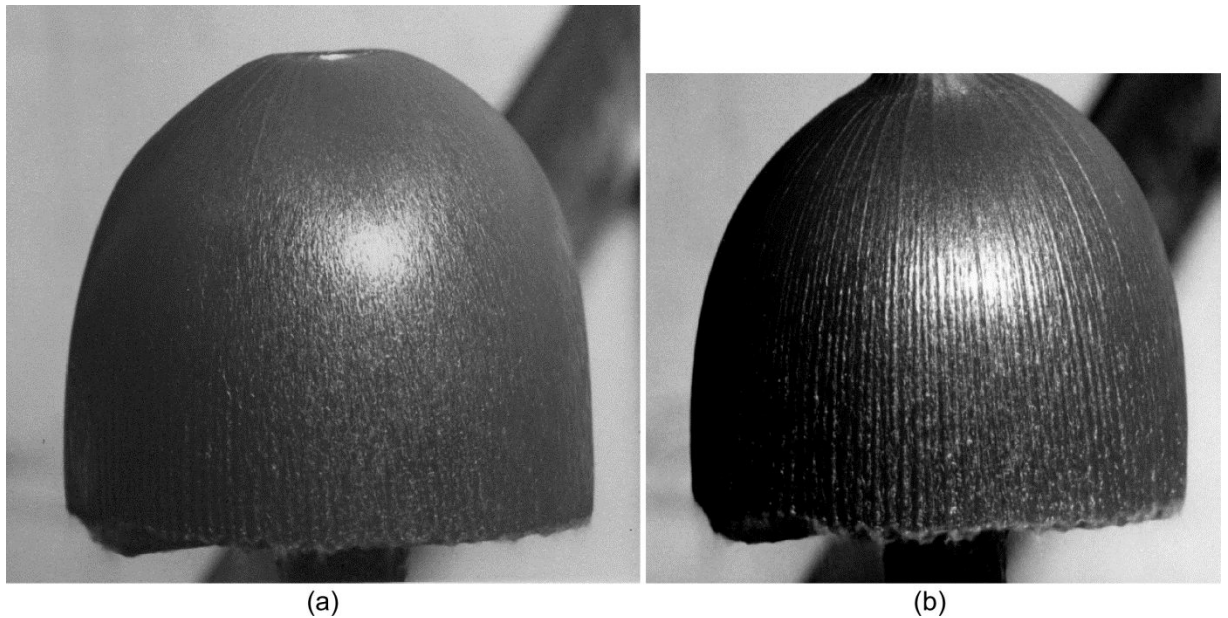


Fig. 4 -(a) Striations begin to develop slightly below the critical Reynolds number of 140,000 (b) are prominent above this Reynolds number. Striations are readily counted in the stagnation region and at the hemisphere- cylinder transition cross-section.

The observed striations are azimuthally periodic, with their relatively sharp peaks and flat valleys similar to the striations seen on stony meteorites. They clearly follow the ambient flow streamlines, indicating that they are driven by local shear stresses at the flow-oil interface. Photos of the model taken during a test were used to estimate the number visible close to the stagnation point, at the hemisphere-cylinder transition, and at the trailing edge of the cylinder.

The observed striations are azimuthally periodic, with their relatively sharp peaks and flat valleys similar to the striations seen on stony meteorites. They clearly follow the ambient flow streamlines, indicating that they are driven by local shear stresses at the flow-oil interface. Photos of the model taken during a test were used to estimate the number visible close to the stagnation point, at the hemisphere-cylinder transition, and at the trailing edge of the cylinder.

IV. Phenomenological Model

While G-T instabilities might be the origin of turbulent fluctuations observed in stagnation regions, they may also be viewed as quasi-organized structures embedded in the boundary layer that act to bring fluid elements with higher velocities and enthalpies closer to the surface than would occur in an undisturbed laminar boundary layer. As a result, the temperature gradient in the boundary layer increases dramatically in the “valleys” and decreases as dramatically on the adjacent “ridges” (i.e., longitudinal striations). The surface temperature in each zone depends on a balance between the mass removal rate and any thermal conduction to the interior (or phase change). The melt removal or “ablation” rate is highest in the valleys, where the heat transfer rate and resulting surface temperature are sufficient to permit oil (or silicates in stony meteorites) to flow and be removed by the interfacial shear stresses. Viscosity being highly temperature dependent [3] in both materials, small differences in surface temperature will have a dramatic effect on the maximum interface velocity, when boundary layer and molten layer shear stresses equilibrate.

Counter-rotating vortices will scavenge material from the valleys and add it to the ridges as it is swept downstream. The scavenged material will be at a higher temperature than interior (frozen) temperatures, reducing heat transfer to, and ablation of, the ridges. The heat transfer rate is reduced by the upward vortical flow, and the molten layer forming the ridges should be thicker than in the valleys, thereby reducing conduction to their interiors. This suggests amplification of ridge formation. With material continuously added to the ridges, it might explain the remarkable stability of longitudinal structures far downstream of the stagnation point. It is also consistent with Figs. 1, 3d, and 4, which indicate wide and shallow valleys and sharp ridges driven by twin counter-rotating vortices that are stretched and intensified by conservation of angular momentum.

V. Comparison of Lafayette Stone Striations with G-T Model

It is first noted that drag and deceleration scale with the square of the flight velocity, while heat transfer rates scale as the cube. Peak re-entry heating occurs earlier than peak deceleration by many kilometers in altitude, the difference depending on a meteorite's mass / drag area and re-entry angle. This suggests that the surface temperature and molten layer responsible for the observed striations on a meteorite may "freeze" before the peak deceleration altitude that would induce L-T instabilities, as observed by Feldman [2]. It is also noted that the minimum L-T wavelength predicted to exist for only several seconds in the flight trajectory is 0.5 cm, or $\lambda/R = 0.10$, approximately twice the ratio on the Lafayette meteorite and in the laboratory simulation.

Following Feldman [2], we consider the re-entry of a meteorite at a Mach number $M = 22$, and estimate the relevant parameters for striation formation, its post-shock gas velocity, density and viscosity. At 20 Km, the atmospheric pressure is 1/14 that at sea level, the post-shock Mach Number is 0.4, and the air density six times ambient. The stagnation pressure is then approximately 1.2 atm. While viscosity is relatively insensitive to temperature [3], velocity scales with the sound speed, which increases as the square root of translational temperature. The post-shock gas translational temperature is limited by vibrational relaxation, molecular dissociation and ionization, depending on flight Mach number, but is at least an order-of- magnitude higher than ambient for the assumed trajectory. The post-shock velocity is then at least three times laboratory test velocities. Including the difference in diameters of the Lafayette stone and laboratory model (10 cm compared to 5 cm), the post-shock Reynolds number is somewhat higher than the maximum test values. Therefore, the laboratory tests simulate striation formation at altitudes above 20 Km, where re-entry heating is close to its maximum. Atmospheric re-entry at higher velocities will result in higher post-shock velocities, but equilibration of gas properties will constrain the Reynolds number, boundary layer thickness and striation wavelength.

There are approximately 100 +/- 10 striations visible on the face of the Lafayette stone (Fig. 1). From Fig. 3d and two additional tests, we can also count approximately 50 +/- 5 striations visible at the trailing edge, or approximately 100 in total. With N the total number of visible striations, the ratio of striation wavelength to model radius, $\lambda/R = \pi/N$, is approximately 0.06, compared to 0.03 predicted by Eq. (2) for planar stagnation regions. Measurement of the number of striations at a model cross-section near the stagnation point and at the hemisphere-cylinder

transition reveal that λ/R is remarkably constant at 0.055 ± 0.005 , with additional vortex pairs generated downstream of the stagnation point as the original pairs diverge. This spreading of vortex pairs suggests that in place of either Eq. (1) or Eq. (2) an improved semi-empirical scaling approximation for striation spacing would be $\lambda/R \sim 20 \text{Re}^{-1/2}$.

VI. Summary

The existence of secondary flow structures resulting from a Görtler-Taylor instability in the stagnation flow boundary layer of two-dimensional (planar) blunt bodies has been accepted for many years and has led to further research on its role as a precursor to stagnation region turbulence. The analogous instability in axially symmetric stagnation point boundary layers has received much less attention. However, evidence of an instability and the formation of vortex pairs that are azimuthally periodic has been seen experimentally via induction of periodic heat transfer and shear effects in frozen oil models of hemisphere-cylinders exposed to a transonic free jet. These experiments were performed as a simulation of the atmospheric re-entry of small, stony meteorites that exhibit longitudinal striations originating at the stagnation point. Measured striation wavelengths are consistent with those observed on the Lafayette stone, and a scaling relationship with flight conditions is developed. The observed wavelength/radius ratios are also a factor of two smaller than the minimum ratio predicted for L-T instabilities at peak heating re-entry conditions [2]. Since post-shock Reynolds number scales as N^2 , further analysis of these azimuthally periodic structures might reveal unobserved flight trajectories of recovered stony meteorites. Related studies might also provide an explanation for similar structures exhibited by volcanic ejecta².

Acknowledgements

This research was supported by the U.S. Air Force under contracts AF 30 (602) 2083, 2393 and 2968 in the Graduate Division of New York University. The author wishes to acknowledge his advisor, Prof. C.K. Chu, and the early encouragement he received from the late Prof. H. Görtler.

² private communication from an anonymous reviewer.

References

- [1] Feldman, S., "On the hydrodynamic stability of two viscous incompressible fluids in parallel uniform shearing motion," *J. Fluid Mech.*, 2, 1957, pp. 343-370.
- [2] Feldman, S., "On the instability theory of the melted surface of an ablating body when entering the atmosphere," *J. Fluid Mech.*, 3, 1958, pp. 131-155.
- [3] Bethe, H. & Adams, M.C., "A theory for the ablation of glassy materials," *J. of the Aero/Space Sciences* 26(6), 1959, pp. 321-350.
- [4] Williams, D.T., "Flow in pits of fluid-dynamic origin", *AIAA Journal*, Vol.1, No.10, 1963, pp.2384-2385.
- [5] Tobak, M., "Hypothesis for the origin of cross-hatching", *AIAA Journal*, Vol.8, No.2, 1970, pp.330-334.
- [6] Swigart, R., "Cross-hatching studies-a critical review", *AIAA Journal*, Vol.12, No. 10, 1974, pp.1301-1318.
- [7] Stock, H., "Surface patterns on subliming and liquefying ablation materials", *AIAA Journal*, Vol. 13, No. 9, 1975, pp.1217-1223.
- [8] Petitjeans, P. and J-E Westfried, "Spatial evolution of Goertler instability in a curved duct of high curvature", *AIAA Journal*, Vol. 34, No. 9, 1996, pp. 1793-1800.
- [9] de Luca, L., Cardone, G., Aymer de la Chevalerie, D., Fonteneau, A., "Goertler instability of a hypersonic boundary layer," *Experiments in Fluids*, 16(1), 1993, pp. 10-16.
- [10] Sescu, A., Alaziz, R. and Afsar, M., "Control of Gortler vortices in high-speed boundary layers," 2018 AIAA Aerospace Sciences Meeting, Kissimmee, FL.
- [11] Floryan, J.M. On the Görtler Instability of Boundary Layers. *Progress in Aerospace Sciences*, v. 28, 1991, 235 – 271.
- [12] Saris, W.S. Görtler Vortices. *Annual Review of Fluid Mechanics* 1994 26:1, 379-409
- [13] Hall, P., Malik, M.R., & Poll, D.I.A.(1984) On the stability of an infinite sweep attachment line boundary layer. *Proc.R.Soc.Lond.A*, 395, pp.229-245.
- [14] Le Duc, A, Sesterhenn, J., & Friedrich, R. Instabilities in compressible attachment - line boundary layers, *Physics of Fluids* 18, 044102 (2006)

- [15] Smith, M.C. and Kuethe, A.M., "Effects of turbulence on laminar skin friction and heat transfer," *Physics of Fluids*, 1966, 9, p. 2337.
- [16] Kestin, J. and Wood, R.T., "Enhancement of stagnation-line heat transfer by turbulence," *Prog. Heat Mass Transfer*, 1969, 2, p. 249.
- [17] Kestin, J. and Wood, R.T., "On the stability of two-dimensional stagnation flow," *J. Fluid Mech.*, 44(3), 1970, pp. 461-479.
- [18] Wilson, S.D.R. and Gladwell, I., "The stability of a two-dimensional stagnation flow to three-dimensional disturbances," *J. Fluid Mech.*, 84(3), 1978, pp. 517-527.
- [19] Schlichting, H., "Boundary Layer Theory," (7th Edition, translated by J. Kestin), McGraw-Hill Book Co., New York, 1979, pp. 526-528, 533, 579-583.
- [20] Legner, H. H. and Finson, M. L., "On the stability of fine-scaled turbulent free shear flows", *J. Fluid Mech.*, 1980, 100(2), pp. 303-319.